TEST CASE: Scattering properties of two anomalous reflectors

A. Díaz-Rubio,[(1)] S. Kosulnikov,[(1)] A.V. Osipov,[(2)] S.A. Tretyakov[(1)]

(1) Department of Electronics and Nanoengineering, Aalto University, Aalto, Finland

(2) Microwaves and Radar Institute, German Aerospace Center, Wessling, Germany

Abstract

Anomalous reflectors scatter the incident electromagnetic wave not only in the specular direction but rather in the directions specified by their structure. Two such reflectors have been designed and manufactured at Aalto University [1] by using two different designs, referred to as "conventional phase gradient" (CFG) and "non-local implementation" (NLI). The reflectors have been realized as MTM-FSS rectangular plates and experimentally tested in the frequency range between 6 GHz and 9 GHz at the premises of Aalto University and German Aerospace Center. Contributors to the test case are invited to compute the *S* parameters of the corresponding planar periodic interfaces, the field distributions near the interface and bistatic scattering cross sections of the reflectors.

1. *Definition of the Geometry and the Material Parameters*

The reflectors (Fig. 1 and Fig. 2) are realized as copper-backed dielectric planar sheets with periodic patterns of copper inclusions on top of the sheet (PCB). The patterns are symmetric with respect to the *y* coordinate but non-symmetric in the *x* direction. The convention about the direction of the *x* axis is assumed throughout.

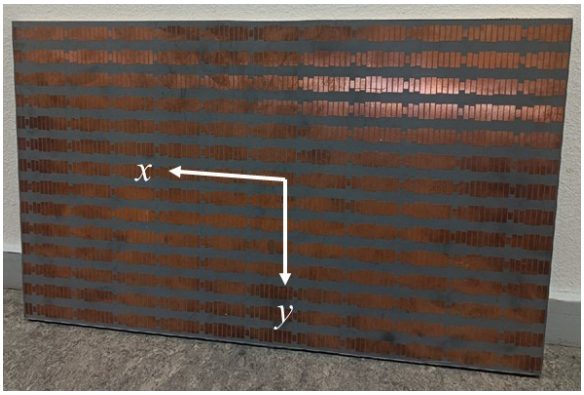

Fig. 1: Non-local implementation

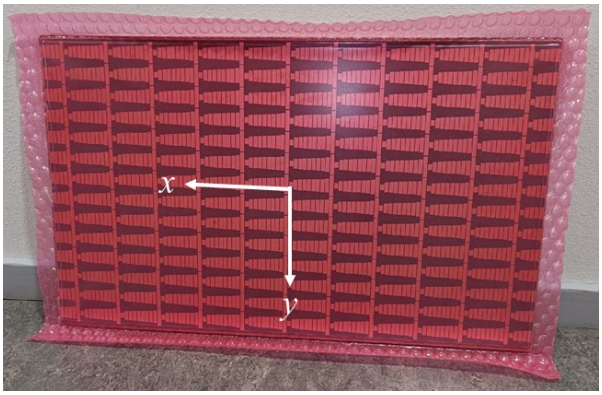

Fig. 2: Conventional phase gradient reflector (covered with a protective foil)

The plates are 11 x 14 arrays of unit cells with the dimensions $D_x = 39.9067$ mm, $L_x = 438.9737$ mm, $D_y = 18.75$ mm and $L_y = 262.5$ mm (Fig. 3). The coordinate frame is chosen such that the plates occupy the region: $-L_x/2 \leq x \leq L_x/2$, $-L_y/2 \leq y \leq L_y/2$. The thickness of the dielectric material is equal to $t_{\text{diel}} = 1.575$ mm, and that of the copper strips is $t_{\text{copper}} = 35$ μm. The material parameters of the involved media are summarized in Table 1.

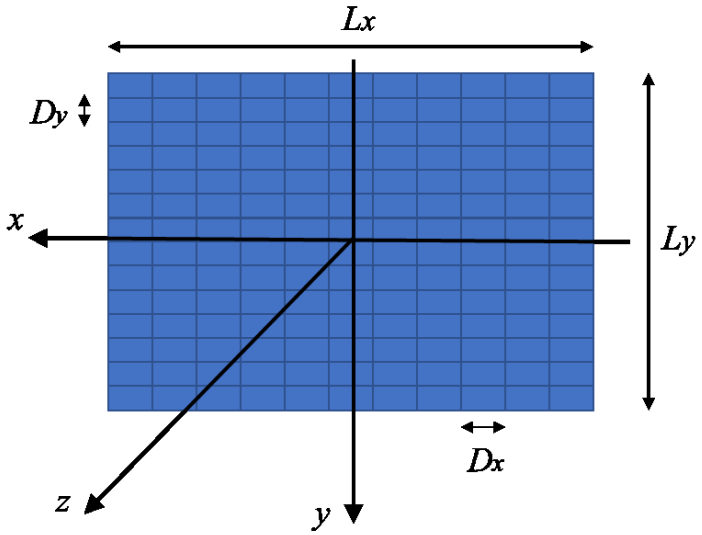

Fig. 3: Coordinate frame, the arrangement of unit cells and the notation for the dimensions of the plates and unit cells

Table 1: Material parameters: relative dielectric and magnetic constants, conductivity and the loss tangent of the involved media

ε_{air}	1.0006
μ_{air}	1.0000004
σ_{copper}	5.8 x 10^7 S/m
μ_{copper}	0.999991
$\varepsilon_{\text{diel}}$	2.2
μ_{diel}	1
$\delta_{\text{diel}}^{\text{Loss.tan}}$	0.0009

The unit cells of both structures consist of 10 copper strips of the same width l_x in the x direction but with varying lengths $l_{y,n}$ in the y direction ($n = 1,2,\dots,10$). The strips are separated by the distance x_{offset} from the upper and lower boundaries of the unit cell and by the distance $2x_{\text{offset}}$ from the neighbouring strips. The values of the design parameters and the views of the unit cells are given in Fig. 4 for the non-local implementation and in Fig. 5 for the conventional phase-gradient design. The CAD datasets in the formats DXF and AEDT are available.

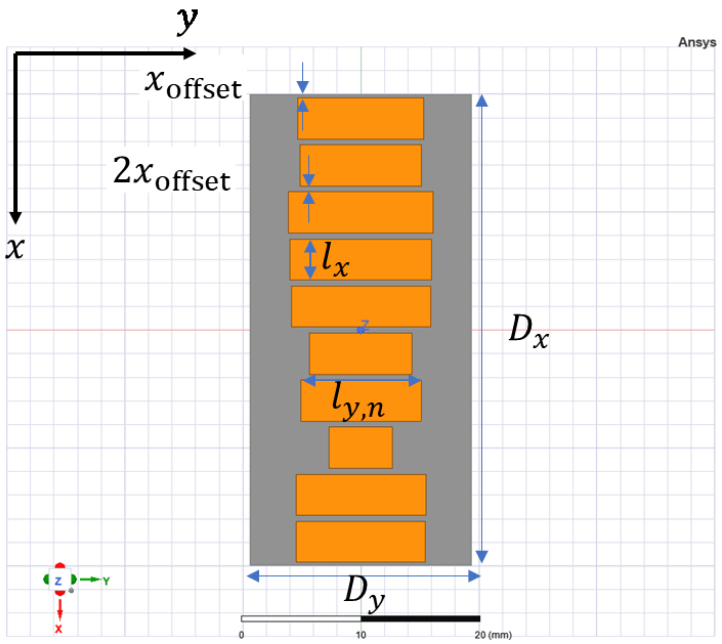

D_x	39.9067 mm
D_y	18.75 mm
l_x	3.49067 mm
$l_{y,1}$	10.7 mm
$l_{y,2}$	10.3 mm
$l_{y,3}$	12.3 mm
$l_{y,4}$	12.0 mm
$l_{y,5}$	11.8 mm
$l_{y,6}$	8.7 mm
$l_{y,7}$	10.2 mm
$l_{y,8}$	5.4 mm
$l_{y,9}$	11.0 mm
$l_{y,10}$	10.9 mm
x_{offset}	0.25 mm

Fig. 4: The structure and the design parameters of a unit cell of the non-local implementation

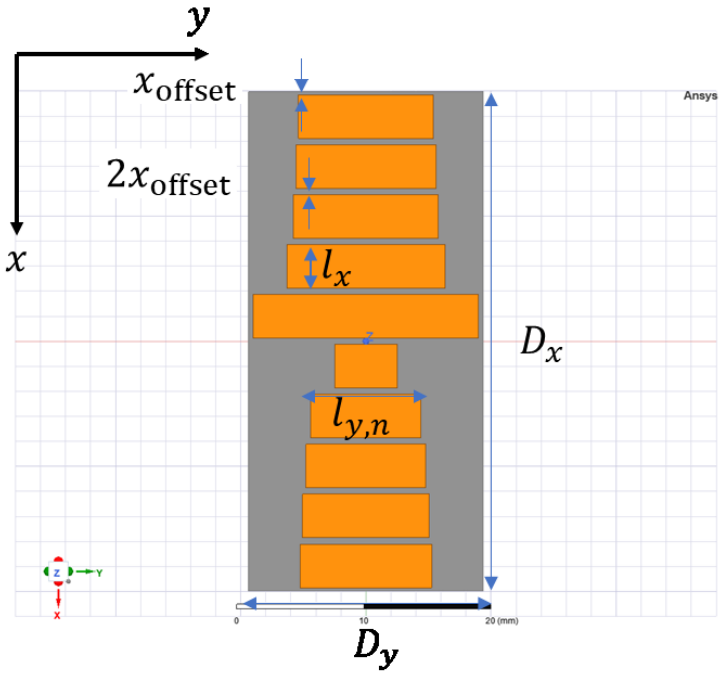

D_x	39.9067 mm
D_y	18.75 mm
l_x	3.49067 mm
$l_{y,1}$	10.7778 mm
$l_{y,2}$	11.1717 mm
$l_{y,3}$	11.5657 mm
$l_{y,4}$	12.6162 mm
$l_{y,5}$	18.0 mm
$l_{y,6}$	5.0 mm
$l_{y,7}$	8.8081 mm
$l_{y,8}$	9.596 mm
$l_{y,9}$	10.1212 mm
$l_{y,10}$	10.5152 mm
x_{offset}	0.25 mm

Fig. 5: The same as in Fig. 4 but for the conventional phase-gradient design

2. Simulation Tasks

2.1 Reflection Coefficient of Infinite Planar Periodic Arrays

Reflection coefficient (S_{11}) of infinite planar periodic arrays, which are built from the unit cells shown in Fig. 4 (non-local implementation) and in Fig. 5 (conventional phase gradient), is to be simulated in the frequency range between 6 GHz and 9 GHz with the step 0.01 GHz. The excitation is a plane wave normally incident on the arrays and polarized along the *y* axis. The goal is to determine the frequency f_0, at which $|S_{11}|$ has a minimum. The minimum is expected to be close to 8 GHz for both samples.

Sub-task code	Polarization of the incident field	Reflector
2.1.1	*y*	NLI
2.1.2	*y*	CPG

2.2 Near-field Scan: Fields in the Infinite-plane Approximation

Scan of the field components E_x, E_y, H_x and H_y over a unit cell along the middle line $-D_x/2 \leq x \leq D_x/2$, $y = D_y/2$ and $z = h$, where $h = 10$ mm, with the step $\Delta x = \frac{D_x}{100} = 0.399067$ mm, i.e. at the points $x_m = -D_x/2 + (m-1)\Delta x$ with $m = 1,2,\dots,101$. The incoming plane wave at the frequency f_0, polarized along the *y* axis, is incident at a right angle to the surface of the arrays. For both reflectors.

Sub-task code	Polarization of the incident field	Reflector
2.2.1	*y*	NLI
2.2.2	*y*	CPG

2.3 Near-field Scan: Exact Fields

Scan of the components of E_x, E_y, H_x and H_y over the whole plate along the line $-7D_x \leq x \leq 7D_x$, $y = D_y/2$ and $z = h$, where $h = 10$ mm, with the step $\Delta x = \frac{D_x}{100} = 0.399067$ mm such that the *x* coordinates of the sampling points are given by the formula: $x_m = -7D_x + (m-1)\Delta x$ with $m = 1,2,\dots,1401$ (Fig. 6). The plane electromagnetic wave polarized along the *y* axis is normally incident on the surface of the reflectors at the frequency f_0. For both designs.

A comparison between 2.2 and 2.3 will show the influence of the edges of the plates on the current distributions induced by the incident wave on the reflectors.

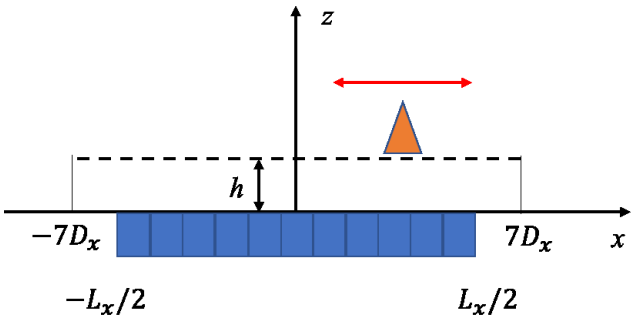

Fig. 6: Configuration assumed in section 2.3

Sub-task code	Polarization of the incident field	Reflector
2.3.1	*y*	NLI
2.3.2	*y*	CPG

2.4 *Bistatic Scattering Cross Section at a Fixed Frequency and Broadside Illumination*

For a plane wave, polarized along the y axis and normally incident on the surface of the reflectors, the bistatic scattering cross section in the x-z plane with the zenith angle θ varying in the interval $-90° \leq \theta \leq 90°$ with the step $\Delta\theta = 1°$ is to be computed at the frequency $f = f_0$ (see section 2.1). The zenith angle $\theta = 0$ corresponds to the incidence in the negative z direction, $\theta = -90°$ along the x axis and $\theta = 90°$ in the negative direction of the x axis (Fig. 7). Computations with the exact surface currents and with the currents in the infinite plane approximation for both designs and for an equally large PEC plate are to be conducted. The goal consists in the determination of the positions of the scattering maxima.

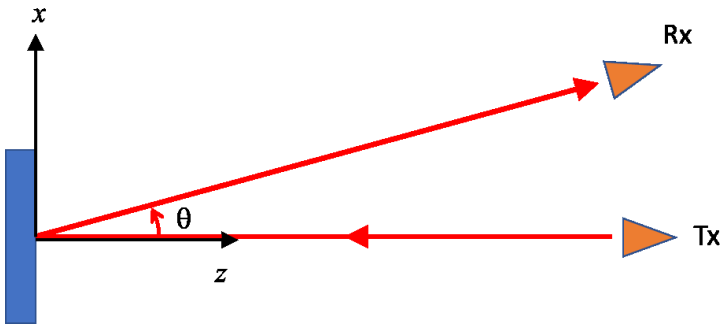

Fig. 7: Bistatic configuration assumed in section 2.4

Sub-task code	Polarization of the incident field	Reflector	Method
2.4.1	*y*	PEC	Exact currents
2.4.2	*y*	NLI	Infinite-plane approximation
2.4.3	*y*	NLI	Exact currents
2.4.4	*y*	CPG	Infinite-plane approximation
2.4.5	*y*	CPG	Exact currents

2.5 *Bistatic Scattering Cross Section at Oblique Illumination*

At the frequency $f = f_0$, bistatic scattering cross section is to be computed for fixed positions of the transmitter and receiver, both located in the *x*-*z* plane and separated by the angle $\beta = 70°$. (Fig. 8). Computations are to be conducted for the varying orientation angle ϕ of the reflectors (rotation around the *y* axis) such that $-20° \leq \phi \leq 90°$ with the step $\Delta\phi = 1°$, where $\phi = 0$ corresponds to the broadside illumination of the plate, $\phi = -20°$ to the *x* axis pointing to the receiver and $\phi = 90°$ to the illumination along the *x* axis. The incident wave is polarized in the *y* direction.

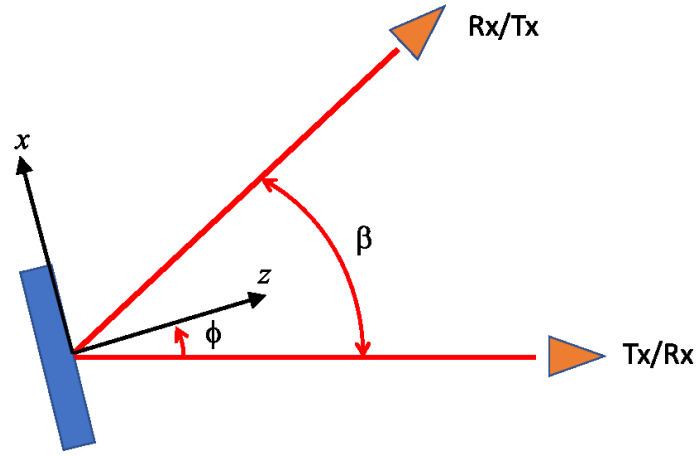

Fig.8: Bistatic configurations assumed in section 2.5

Sub-task code	Polarization of the incident field	Reflector	Method
2.5.1	*y*	PEC	Exact currents
2.5.2	*y*	NLI	Infinite-plane approximation
2.5.3	*y*	NLI	Exact currents
2.5.4	*y*	CPG	Infinite-plane approximation
2.5.5	*y*	CPG	Exact currents

The computations are to be repeated for the interchanged positions of the transmitter and receiver, in which case the *z* axis points to the receiver when $\phi = 0$ and to the transmitter when $\phi = 70°$ (Fig. 8).

Sub-task code	Polarization of the incident field	Reflector	Method
2.5.6	*y*	PEC	Exact currents
2.5.7	*y*	NLI	Infinite-plane approximation
2.5.8	*y*	NLI	Exact currents
2.5.9	*y*	CPG	Infinite-plane approximation
2.5.10	*y*	CPG	Exact currents

3. *Data Formats*

The results are to be stored in ASCII files, named as

- *test_case_xxx_2-1-1_CONTRIBUTOR_NAME.txt*
- *test_case_xxx_2-1-2_CONTRIBUTOR_NAME.txt*

- *test_case_xxx_2-2-1_CONTRIBUTOR_NAME.txt*
- *test_case_xxx_2-2-2_CONTRIBUTOR_NAME.txt*

- *test_case_xxx_2-3-1_CONTRIBUTOR_NAME.txt*
- *test_case_xxx_2-3-2_CONTRIBUTOR_NAME.txt*

- *test_case_xxx_2-4-1_CONTRIBUTOR_NAME.txt*
- *test_case_xxx_2-4-2_CONTRIBUTOR_NAME.txt*
- *test_case_xxx_2-4-3_CONTRIBUTOR_NAME.txt*
- *test_case_xxx_2-4-4_CONTRIBUTOR_NAME.txt*
- *test_case_xxx_2-4-5_CONTRIBUTOR_NAME.txt*

- *test_case_xxx_2-5-1_CONTRIBUTOR_NAME.txt*
- *test_case_xxx_2-5-2_CONTRIBUTOR_NAME.txt*
- *test_case_xxx_2-5-3_CONTRIBUTOR_NAME.txt*
- *test_case_xxx_2-5-4_CONTRIBUTOR_NAME.txt*
- *test_case_xxx_2-5-5_CONTRIBUTOR_NAME.txt*
- *test_case_xxx_2-5-6_CONTRIBUTOR_NAME.txt*
- *test_case_xxx_2-5-7_CONTRIBUTOR_NAME.txt*
- *test_case_xxx_2-5-8_CONTRIBUTOR_NAME.txt*
- *test_case_xxx_2-5-9_CONTRIBUTOR_NAME.txt*
- *test_case_xxx_2-5-10_CONTRIBUTOR_NAME.txt*

where *xxx* is the number of the test case (not assigned yet), which is followed by the sub-task code. “CONTRIBUTOR_NAME” should be replaced by the name of the contributing institution and, if necessary, followed by a postfix indicating the method used for the simulations, e.g., Contributor1_FDTD, Contributor1_MoM, …

The data files (“*test_case_xxx_2-1-1_...*” and “*test_case_xxx_2-1-2_...*”) for the tasks from section 2.1 should be written in the format:

f Re S_{11} Im S_{11} Abs(S_{11})

where f is the frequency in GHz, S_{11} is the S parameter (ratio of the reflected and incident signals), Re S_{11} and Im S_{11} denote the real and imaginary parts of the S parameter and Abs(S_{11}) is the absolute value of the parameter in dB, i.e. 20 lg(Abs (S_{11})).

The data files ("*test_case_xxx_2-2-1_...*" and "*test_case_xxx_2-2-2_...*") for the tasks from section 2.2 should be written in the format:

x Re E_x Im E_x Re E_y Im E_y Re H_x Im H_x Re H_y Im H_y

where x is the position of the scanning probe in mm and E_x, E_y, H_x and H_y are the field components tangential to the surface of the reflectors.

The data files ("*test_case_xxx_2-3-1_...*" and "*test_case_xxx_2-3-2_...*") for the tasks from section 2.3 should be written in the format:

x Re E_x Im E_x Re E_y Im E_y Re H_x Im H_x Re H_y Im H_y

where x is the position of the scanning probe in mm and E_x, E_y, H_x and H_y are the field components tangential to the surface of the reflectors.

The data files ("*test_case_xxx_2-4-1_...*", "*test_case_xxx_2-4-2_...*", … , "*test_case_xxx_2-4-5_...*") for the subtasks from section 2.4 should be written in the format:

θ σ_θ σ_y

where θ is the zenith angle in degree, σ_θ is the scattering cross section for the θ components of the scattered field in dBsm and σ_y is the scattering cross section for the y component of the scattered field in dBsm (= $10\log_{10}|\sigma|$).

The data files ("*test_case_xxx_2-5-1_...*", "*test_case_xxx_2-5-2_...*", … , "*test_case_xxx_2-5-10_...*") for the subtasks from section 2.5 should be written in the format:

ϕ σ_θ σ_y

where ϕ is the orientation angle of the reflector in degree, σ_θ is the scattering cross section for the θ components of the scattered field in dBsm and σ_y is the scattering cross section for the y component of the scattered field in dBsm.

4 *Additional Information*

Each *.txt* file should be accompanied by an *.info* file, stating additional information relevant for the simulation, e.g., short description of the method used, CPU time, memory usage, number of unknowns, characteristics of simulation hardware (number of cores, processor speed), etc.

5 *Reference*

[1] Ana Díaz-Rubio, Viktar S. Asadchy, Amr Elsakka, Sergei A. Tretyakov (2017), From the generalized reflection law to the realization of perfect anomalous reflectors, *Science Advances*, **3**: e1602714